Effect of twinning and detwinning on the spring-back and shift of neutral layer in AZ31 magnesium alloy sheets during V-bend

Lifei Wang [a,b], Guangsheng Huang [a,*], Tingzhuang Han [a], Ehsan Mostaed [b], Fusheng Pan [a], Maurizio Vedani [b]

[a] *College of Materials Science and Engineering, Chongqing University, Chongqing 400045, China*
[b] *Department of Mechanical Engineering, Politecnico di Milano, 20156 Milan, Italy*

Received 20 June 2014
Accepted 13 December 2014
Available online 24 December 2014

1. Introduction

As the lightest structural metal, magnesium and its alloys have attracted a large number of industrial sectors due to their high specific strength and stiffness [1,2]. However, owing to hexagonal close packed (HCP) structure, magnesium shows a poor formability at room temperature. In other words, since there are limited numbers of available slip systems in magnesium crystals at low temperatures. The Von Mises Criterion requiring at least 5 independent slip systems for plastic deformation of polycrystalline metals to occur which cannot be met and limited ductility is shown [3]. Accordingly, improving the ductility and strength of magnesium alloys through different procedures has been widely investigated. Recently, pre-strain has been found to be a proper method to significantly improve the mechanical properties in magnesium alloys. Song et al. [4] and Xin et al. [5] reported that the $\{10\bar{1}2\}$ twins-induced by pre-rolling could actually split grain crystals and thereby leads to grain refining, improving the mechanical properties of magnesium alloys. Wang and Huang [6] indicated that the twins generated by pre-compression along extrusion direction disappeared after inverse tension which resulted in improvement of plasticity in an AZ31 magnesium alloy. Zhang et al. [7] also proved that the basal texture was weakened by pre-stretch deformation and that the formability of the AZ31 magnesium alloy sheet was improved.

Being one of the most important processing techniques, bending is also known to be affected by the complex springback phenomenon. Besides, during bending, the outer-layer of the sheets is under tensile deformation while the inner-layer will be under compressive deformation. The different deformation modes result in a shift of the neutral layer during bending. For common metals like aluminum, the neutral layer shifts to the inner compressive region. However, for magnesium alloys featuring an HCP structure is opposite. Thus, as reported in the previous research [8], the asymmetry of the deformation mechanism leads to a shift of the neutral layer of the alloy to the outer tensile region. It was also proved that twinning plays an important role on the tension–compression asymmetry [9]. The more frequent the twins, the bigger the tension–compression asymmetry will be. Hence, twinning must have an important effect on the shift of the neutral layer in magnesium alloys during bending. It is well known that detwinning occurs after inverse deformation [10,11] and accordingly, during bending, springback cannot be avoided and an inverse load will be induced, leading to the concurrent detwinning behavior. To the authors' knowledge, detwinning behavior during bending has not been researched so far. In this paper, twins were induced in an AZ31 alloy by different pre-strain (pre-stretch and pre-compres-

* Corresponding author. Tel.: +86 23 65112239; fax: +86 23 65102821.
E-mail address: Gshuang@cqu.edu.cn (G. Huang).

sion) paths and thereafter the effect of pre-strain as well as twinning–detwinning behavior on spring-back and shift of neutral layer during bending of sheets were thoroughly investigated.

2. Experimental procedure

A commercial rolled sheet of AZ31 magnesium alloy (Mg–3 wt.%Al–1 wt.%Zn) having a thickness of 3 mm was annealed at 673 K for 4 h. Rectangular specimens with a width of 30 mm and a length of 100 mm were cut from the annealed sheets. Some of the specimens were then pre-stretched along their rolling direction (RD) by 3% or 5% at a strain rate of 10^{-3} s^{-1} at room temperature. Other specimens with the same size were pre-compressed along RD by 1%, 3%, 5% as well at room temperature. The pre-strained samples were annealed at 200 °C for 2 h. In order to avoid buckling of the sheet during compression, a special mold was designed, as shown in Fig. 1. During compression, standard mineral oil was used as a lubricant.

Samples with 30 mm width and 80 mm length were cut from the pre-strained sheets and subjected to V-bending to an angle of 90° on a CMT6305-300KN electro-mechanical universal testing machine at the temperature of 423 K based on General Administration of Quality Supervision, Inspection and Quarantine of the People's Republic of China (AQSIQ) Standard GB/T GB/T232-2010 [12]. Due to poor formability of the alloy, bending was conducted at 423 K by placing the die and the specimens in a resistance furnace fitted to the testing machine. The V-punch had a radius of 9.3 mm and the initial speed of the punch was set to 10 mm/min. In order to ensure reproducibility of the experiments, for each condition three tests were carried out. In order to keep the same conditions and minimize the effect of unloading time on springback, all the specimens kept 30 s after V-bending before unloading. After V-bending, the thickness of the samples was measured using a universal goniometer. The offset of neutral layer was measured by the coefficient of neutral layer (*k* value). The coefficient (*k*-value) was the standard of offset of neutral layer. The bigger of *k*-value, the further away shifting of neutral layer from geometrical middle layer will be. If *k*-value is less than 0.5, it means neutral layer shift to compressive region during bending. If it exceeds 0.5, neutral layer shifts to the outer tensile region accordingly.

According to a theory of stamping process, the computational formula of the *k* value is given as:

$$k = 0.5\beta^2 - (1-\beta) * R_i/t \quad (1)$$

where k, β, R_i and t are the coefficient of the neutral layer, the coefficient of incrassation, the inside bending radius and the original thickness of the sheet, respectively.

The microstructure of the samples was characterized by optical microscopy and by electron backscatter diffraction (EBSD). The optical microstructure was observed after standard metallographic preparation technique while samples preparation for EBSD consisted in mechanical grinding followed by polishing down to colloidal silica naps. Then, electro-polishing was performed using a solution of 20% nitric acid and 80% methanol with a voltage of 20V for 120 s at temperature of −30 °C. Finally, EBSD measurements were performed on a Zeiss EVO 50 SEM. The EBSD data were processed by an INCA OXFORD crystal software.

3. Results and discussion

Optical micrographs illustrating the microstructure of the AZ31 alloy at different pre-strain levels are shown in Fig. 2. The as-received microstructure consisted of large amount of equiaxial grains with an average size of 18 μm. After 3% PRS and 5% PRS some of the grains appeared to be deformed but no twins emerged. However, a large number of twins were found in the microstructure of PRC samples. The twinning lamellar structure was preserved when annealing below 473 K took place, which is consistent with previous research results [13]. By increasing the level of PRC strain, the volume fraction of twins increased as well, and, especially in 5% PRC samples, almost all the grains contained twins. The (000 2) pole figures of as-received, 3% PRT and 3% PRC samples are depicted in Fig. 3. It can be observed that the as-received AZ31 plate exhibits a typical basal texture. After pre-stretch deformation, the basal texture did not change too much, however, in 3% PRC samples, a texture//RD was induced by twins. According to the EBSD maps, the twinning boundaries are (10−12) twins. It is widely accepted that the {10−12} twinning always occurs when tension is applied along the *c*-axes of most grains or when compression is applied perpendicular to the *c*-axes [14].

The load vs position curves during bending of various pre-strained samples experimentally obtained are shown in Fig. 4. As expected, the bending load increased with pre-strain deformation levels. Comparing the load–position curves in various pre-strained samples in Fig. 4(c), the bending load was higher in the PRC than in the PRT samples, even 1% PRC featured a higher bending load than 5% PRT.

The trend of springback and coefficient of neutral layer (*k-value*) after V-bending to 90° of the pre-strained samples is shown in Fig. 5. The springback value increases with increasing PRT and PRC levels. It is well known that springback is affected by both the elastic modulus and the yield stress of the material [15]. It is supposed that elastic modulus does not vary too much by pre-strain deformation. Bruni et al. [16] indicated that the decrease of springback with the increasing temperature was mainly due to the decrease of flow stress recorded on the load–stroke curves dur-ing bending, and to lower amount to decrease inelastic modulus. As shown in Fig. 4, the flow stress (which is assumed to directly depend on position of the bending load) increased with the increase of PRT and PRC levels, resulting in an improvement in

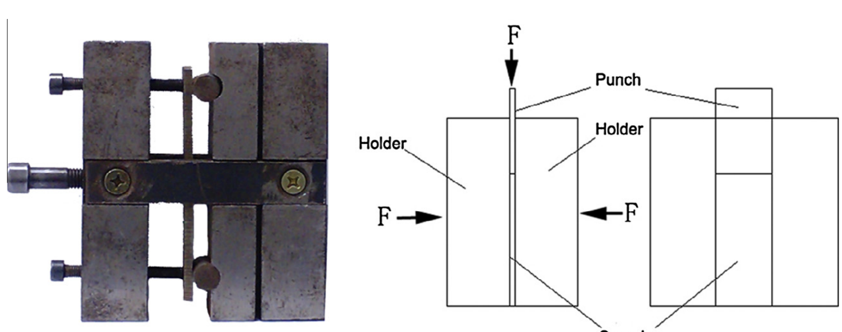

Fig. 1. The sheet compressive mold and sketch map of load.

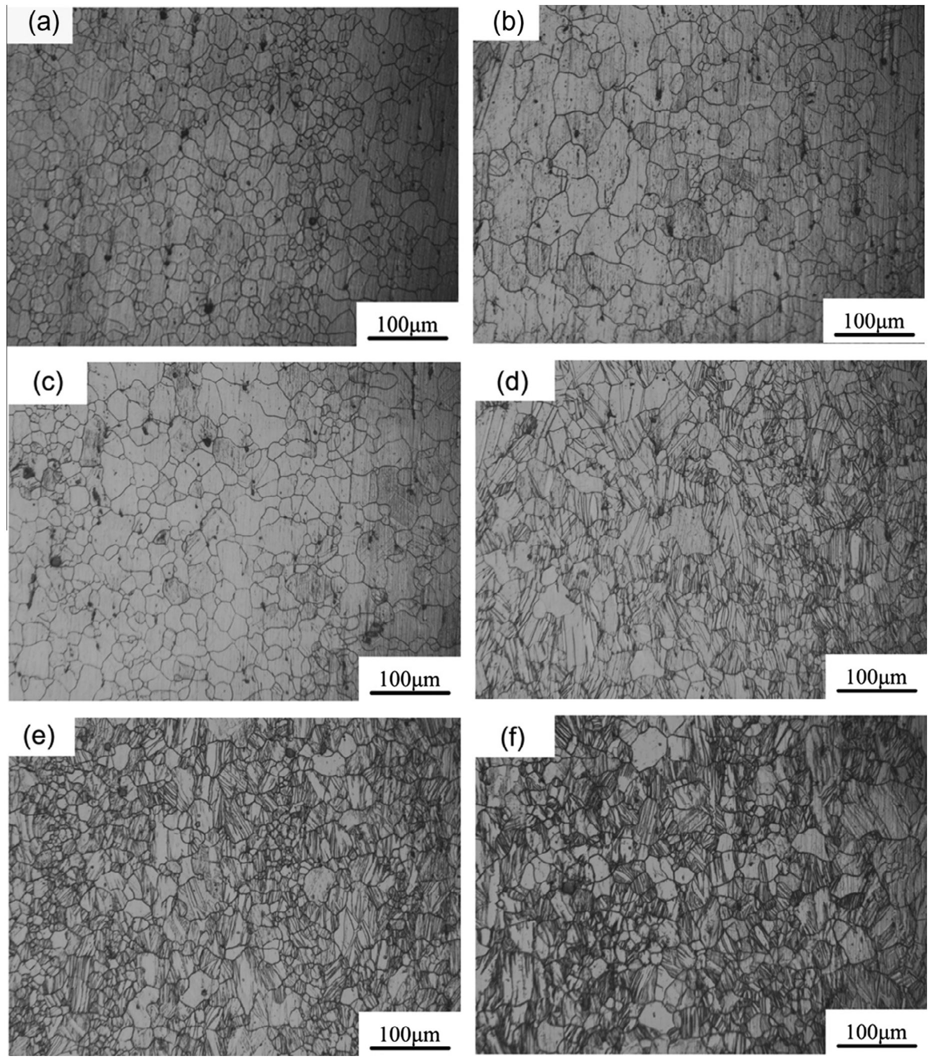

Fig. 2. Optical microstructure of various samples with pre-strain along RD: (a) as-received, (b) PRS 3%, (c) PRS 5%, (d) PRC 1%, (e) PRC 3%, (f) PRC 5%.

the springback. Besides, springback increased after PRT was much larger than that measured after PRC deformation.

The coefficients of neutral layer (*k-values*) given in Fig. 5(b) show that *k-values* decreases not only after PRT but also after PRC deformation. In our previous researches [17], the neutral layer of magnesium alloy shifted to the outer tension region, which was different from the common behavior of other materi-als. This is attributed to the tension/compression asymmetry found in HCP metals. During the bending, the outer region was under tensile deformation, which was dominated by slip-assisted mechanisms. However, the inner region was under compressive deformation which was mainly dominant by {10−12} tensile twinning effects. The differences of deformation mechanisms between two sides resulted in the shift of the neutral layer. Regarding the present phenomenon about *k-value* after pre-strain, it could be supposed that it is related to the transformation of asymmetry deformation mechanism between outer and inner regions during bending.

In order to gain a better understanding about the effects of pre-strain on the tension/compression asymmetry, the microstructural observation on different positions in the bending samples was carried out, as detailed in Fig. 6. Accordingly, the outer, middle and inner regions during V-bending after different PRT and PRC deformation levels are represented in Fig. 7. Moreover, Fig. 8 shows the (0 0 0 2) Pole figures and IPF maps of as-received, 3% PRS and 3%PRC samples in the middle region after bending. It is seen that in the as-received sample many twins are observed in the inner region, while no twins appear in the outer layers. Furthermore, a twinning band is observed in the microstructure at middle thick-ness, which is supposed to be due to the asymmetry of deforma-tion mechanism between the inner and outer layers. According to the EBSD results, the mentioned twins are {10−12} tensile twins and a texture of *c*-axis//RD is developed. As well known, {10−12} twins rotates the crystal lattice by 86° which is nearly parallel to the rolling axis.

The amount twins in the inner region of the bent samples decreased after PRT, as expected. Besides, the volume fraction of twins in 3% PRT samples was lower than that observed in 5% PRT samples since twinning was restrained by PRT deformation during bending in the inner region. From the IPF map of 3% PRT samples in Fig. 8(b), it is seen that the type of twins did not change, still remaining {10−12} twins. Sheng et al. [18] reported that the c/a ratio dropped during straining in the tensile part of the fatigue cycles. Due to the reduction of the c/a ratio in tension and the increase of the same in compression, the distance of tangential strain for twinning during compression was longer after pre-stretch deformation. Moreover, compared with the as-received sample, the resistance to activate twinning increased and thereby,

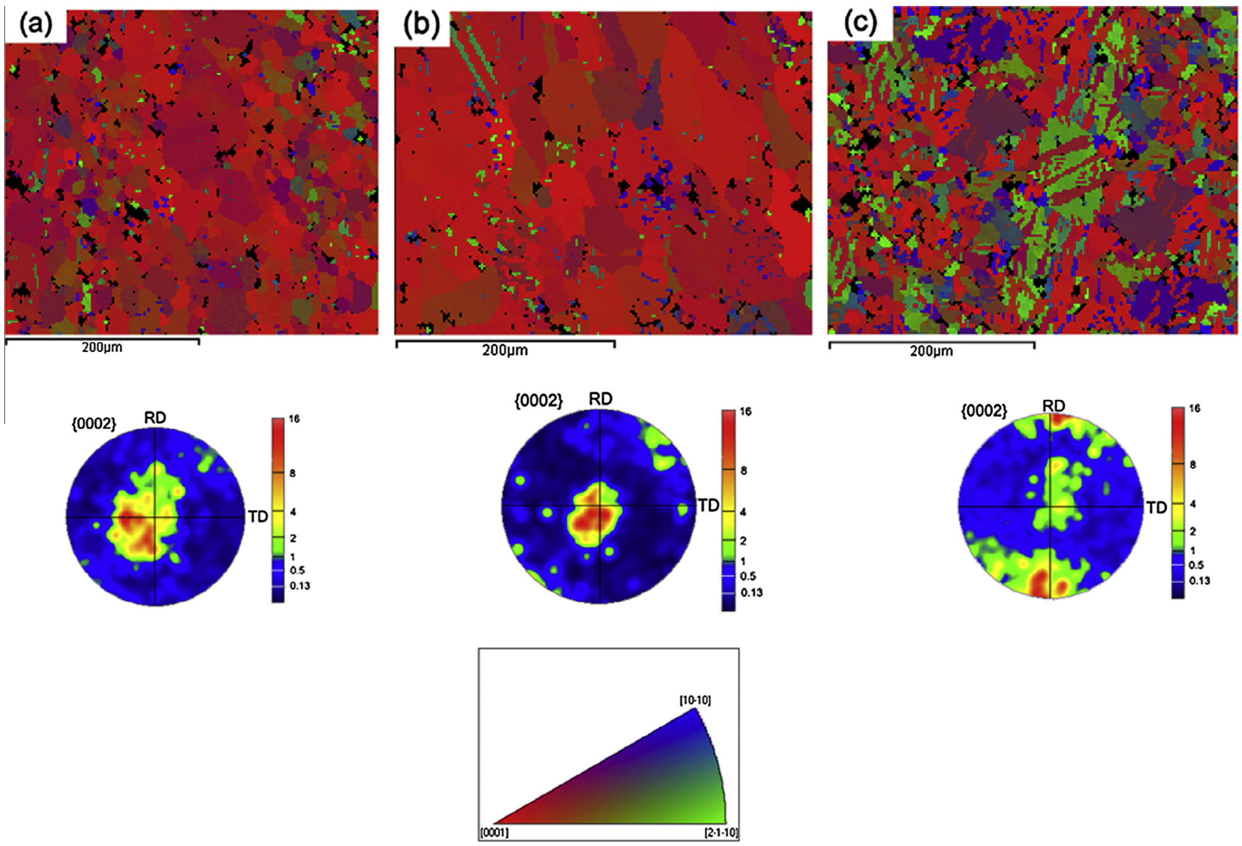

Fig. 3. (0002) pole figures and IPF maps of various samples: (a) as-received; (b) PRS3%; and (c) PRC3%.

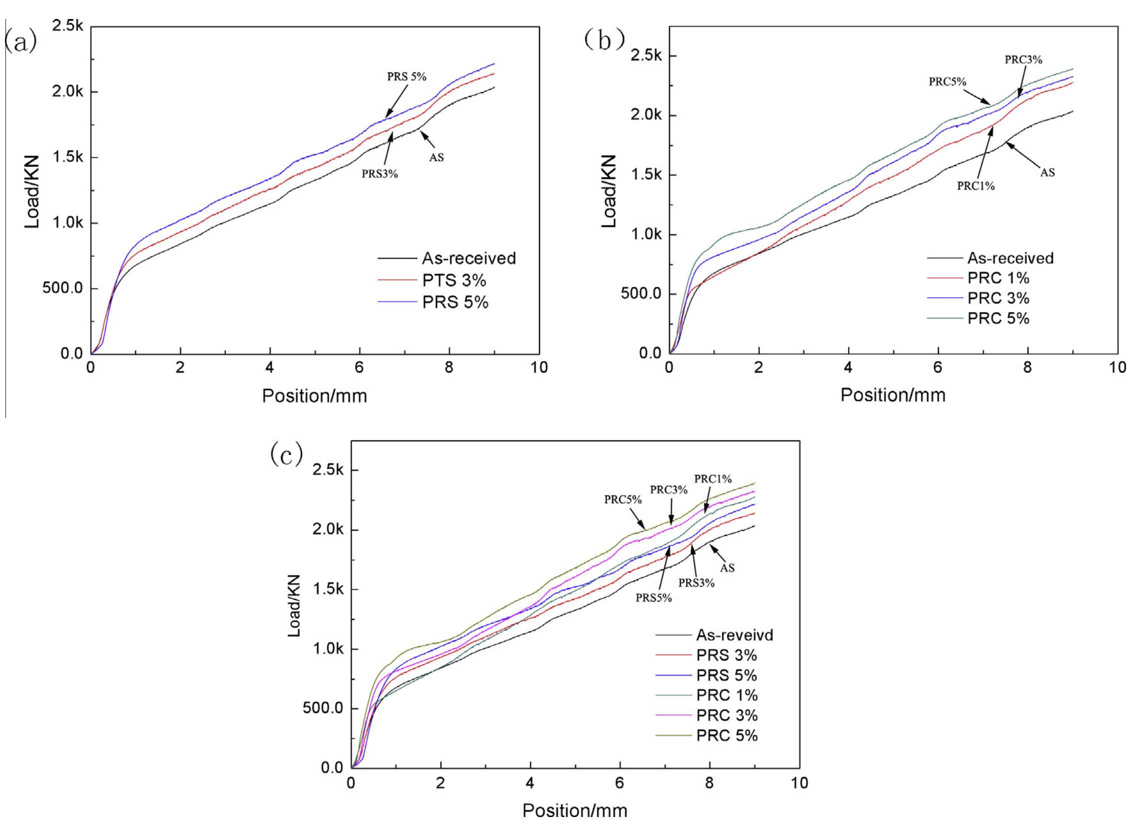

Fig. 4. Load–position curves in various pre-strain samples during V-bending: (a) PRT, (b) PRC, (c) PRT and PRC.

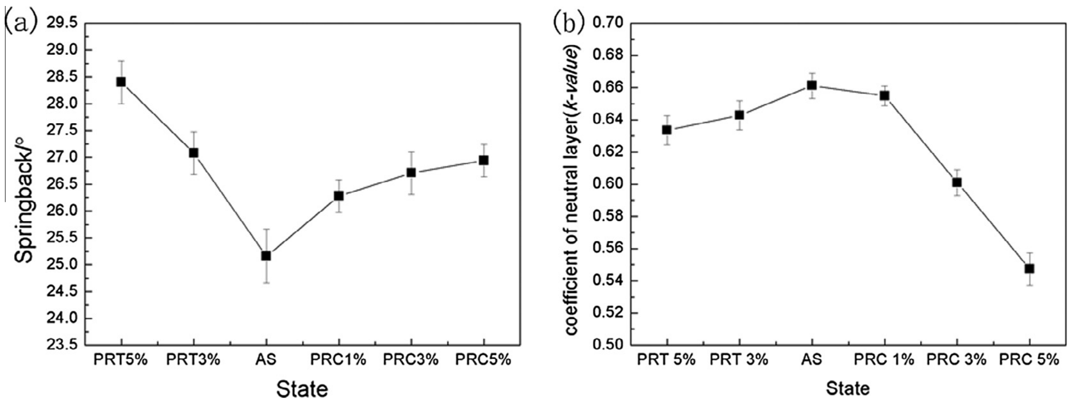

Fig. 5. Effect of pre-strain during V-bending on (a) springback and (b) coefficient of neutral layer.

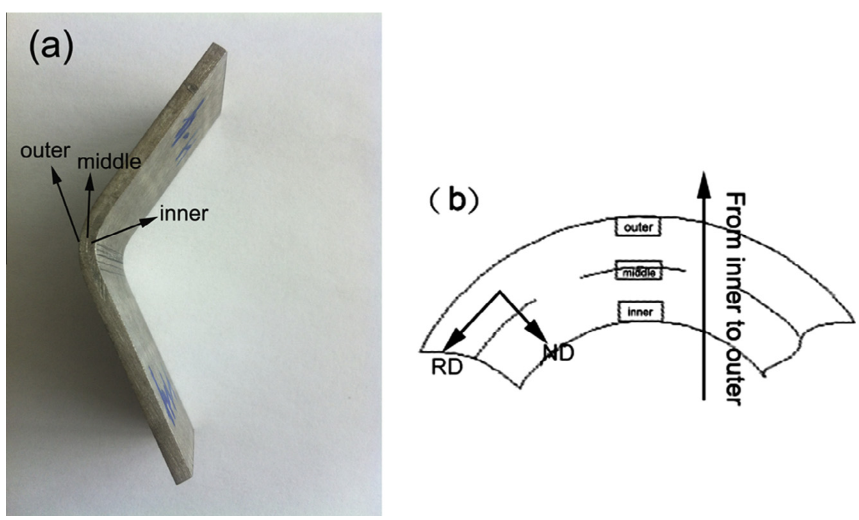

Fig. 6. Measurement positions for microstructure and EBSD analysis in the RD–ND plane: (a) as-received bend sample; (b) schematic diagram of positions.

the amount of twins decreased after PRT. However, as PRT level increases, it is believed that the c/a ratio drops significantly so that it becomes more difficult to activate the twinning mechanism at 5% PRT and a smaller volume fraction of twins appeared in the inner region of the sheet during bending. It is well known that twinning has an important effect on the tension–compression asymmetry of Mg alloys [19,20]. In PRT samples, during bending in the outer region the deformation was dominated by slips, while in the inner compression region {10−12} twinning was dominant. These two regions were separated by a transition zone hereafter called the twin transition band. The larger the volume fraction of twins detected in the microstructure, the bigger the tension–compression asymmetry that is measured. Therefore, not only the asymmetry mechanism in PRT samples during bending decreased, but also the *k*-value decreased, as shown in Fig. 5(b).

After PRC deformation, a large amount of twins were distributed in the microstructure, (Fig. 2). However, as shown in Fig. 7(d–f), during V-bending the twins disappeared in the outer tensile region. Since It is generally accepted that for Mg alloys dynamic recrystallization (DRX) only occurs above 473 K, the disappearance of twins could be reasonably related to detwinning behavior at 423 K [21]. Wu et al. [22] indicated that detwinning happens when the load is on the inverse direction, especially for 1% PRC samples, the detwinning behavior completed thoroughly in the outer region after bending so that all the twins were annihilated and the microstructure was simply composed of equiaxed grains (Fig. 2(d)). Comparing the microstructure of 3% PRC and 5% PRC in Fig. 2(e and f) with the microstructure of the outer region of the bending samples, the volume fraction of twinning lamellas decreased rapidly. Therefore, during the V-bending process the deformation was dominated by detwinning in PRC samples in outer tension region. On the other hand, a large amount of twins was still distributed in the inner region and the volume fraction of twins increased significantly more than it was recorded on PRC samples. It could be concluded that new twins emerged during bending in inner regions and also that in this region the dominated deformation mechanism was still twinning. It was reported that detwinning was very similar to the twinning process however, the detwinning mechanism may require less stress to be activated due to the already existing twins and thereby, no nucleation was needed. In addition, back-stresses engendered by the twinning growth may aid the detwinning process [23]. In PRC samples, the deformation mechanism between inner and outer regions could not be clearly distinguished. As the PRC level increasing, more twins emerged and in turn, more strain and stress was needed to complete the detwinning in the outer region during the bending process. Especially in 5% PRC, detwinning could only be activated just in the outer regions. Accordingly, the asymmetry of deformation mechanism between the inner and outer regions of the samples induced by PRC deformation decreased. As the PRC decreased, the shift of neutral layer decreased at the same time (Fig. 5).

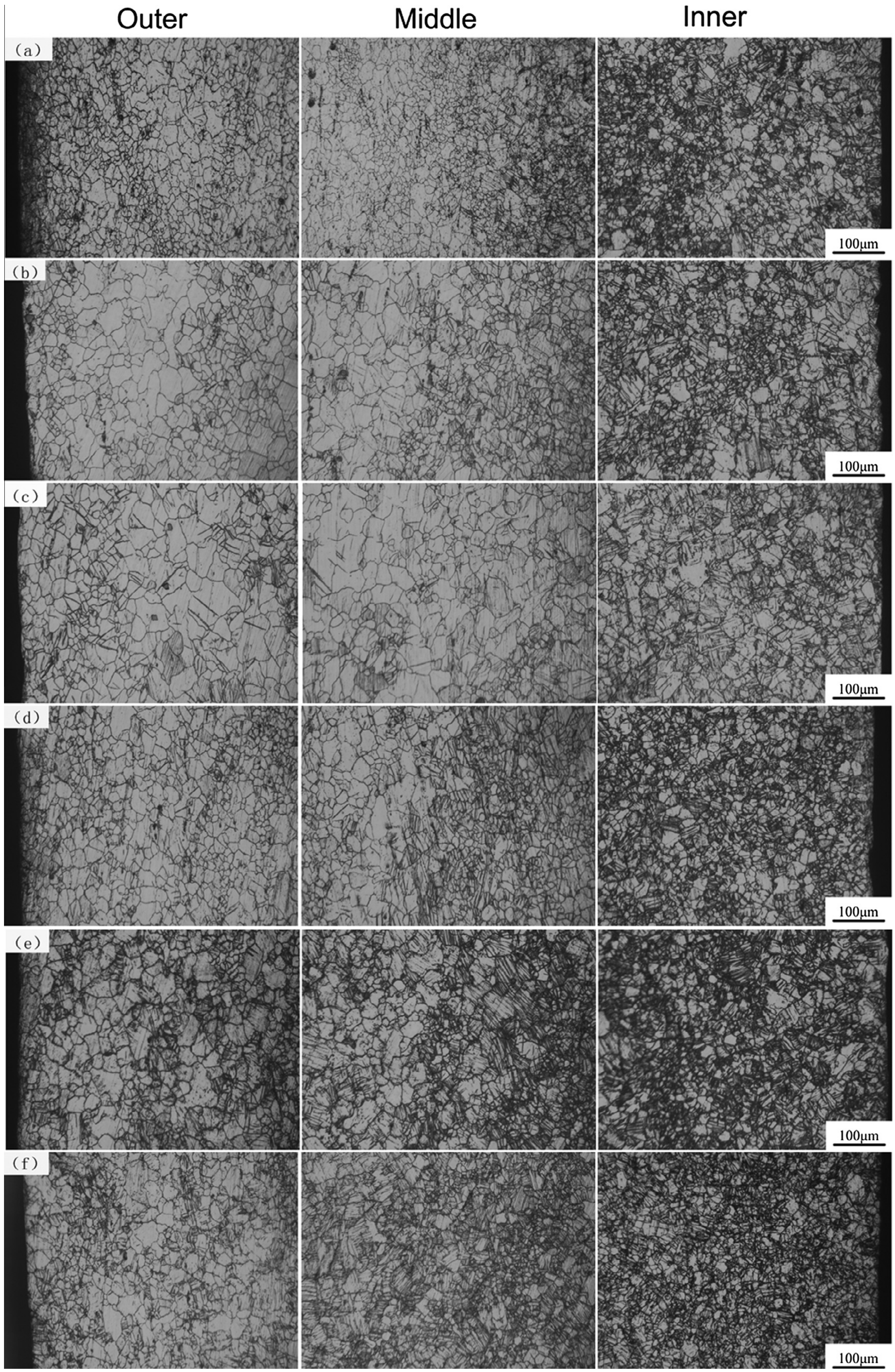

Fig. 7. Optical microstructure of various pre-strain samples of Mg alloy in different regions: (a) as-received, (b) PRT3%, (c) PRT5%, (d) PRC1%, (e) PRC3%, (f) PRC5%.

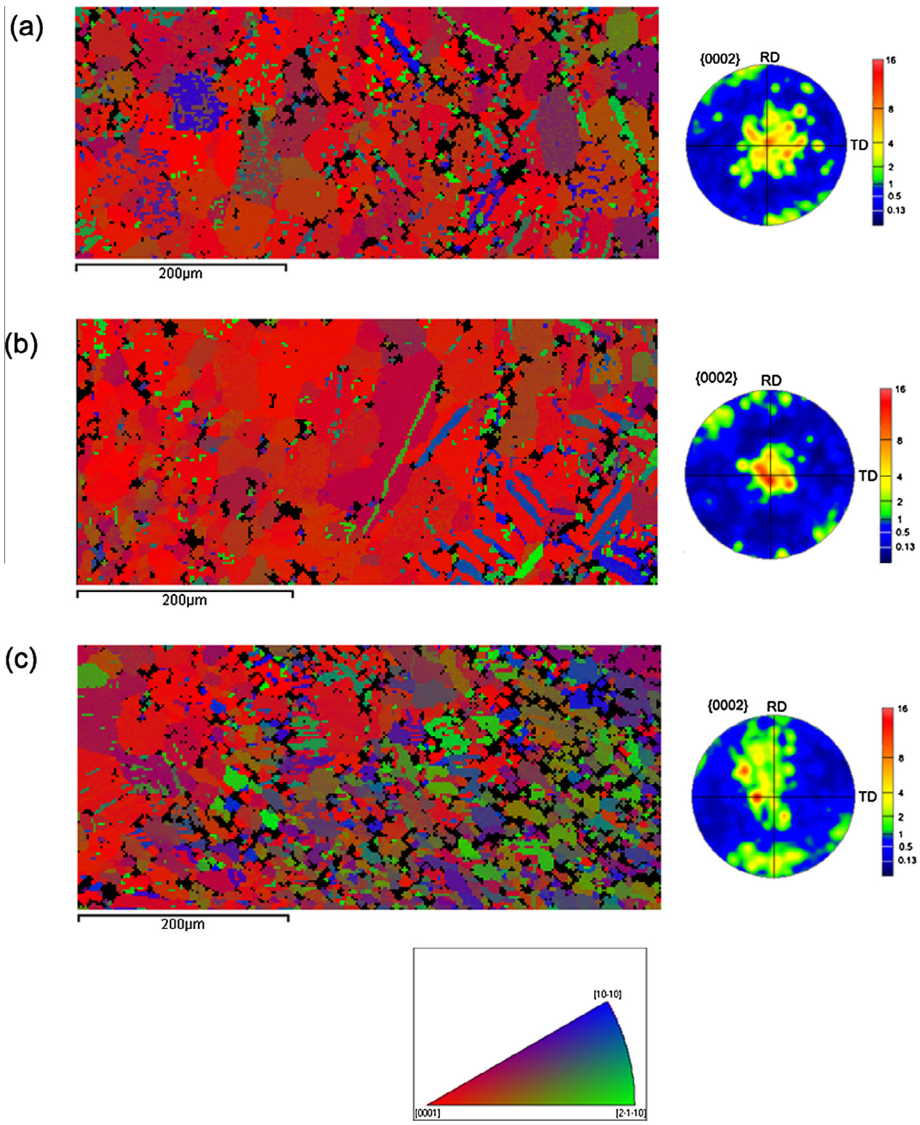

Fig. 8. (0002) pole figures and IPF maps of various samples in the middle region after bending: (a) as-received (b) PRT3% and (c) PRC3%.

Interestingly, the twin transition band was also observed in the middle of PRC samples microstructure, as shown in Figs. 7 and 8. During bending, the effective strain started spreading from the outer and inner layers to the middle region gradually. It is well known that a critical resolved shear stress (CRSS) is needed to activate the twinning. When the stress cannot fit the CRSS, twinning stops and a twinning divide occurs. For PRC samples, the dominated deformation mechanism in the outer regions was observed to be detwinning, while slips played a crucial role in the as-received samples. In other words, detwinning was promoted in the outer region firstly and spread to the middle afterward. When twinning was close to the neutral layer or when the stress was too small implying that CRSS could not be exceeded, detwinning stopped and the twins remained in the microstructure. The higher volume fraction of twins, the more stress and strain is needed to further progress with the detwinning mechanism. In 1% PRC samples, the amount of twins was not significant, suggesting that detwinning had further progressed. In the middle region, one part of the microstructure contained equiaxed grains, while in the other part twins were present. Moreover, the twin transition band was clearly observed in the microstructure. With increase of PRC levels, in 3% PRC sample, the t twin transition band still remained although it was not very evident. Some of the grains completed detwinning, however, the rest of the grains still had the thin twinning variants. In addition, comparing the (000 2) pole figure of 3% PRC sample in Fig. 3(c) with the bending one, it is seen that the texture//RD induced by (10−12) twins weakened. In 5% PRC samples, the twin transition band could not be seen any more and the thin twins distributed in almost every grain in the middle region. This behavior should possibly be attributed to the movement of detwinning further away and locating in the deep outer tension region.

4. Conclusions

The springback and shift of neutral layer of AZ31 sheets were investigated by V-bending at 423 K in the pre-compression and pre-stretch samples deformed to different levels. During bending, the asymmetry of deformation mechanism led to the neutral layer shift toward outer tensile region. Springback and coefficient of neutral layer (*k-value*) increased and decreased, respectively, both in PRS and PRC samples. During bending in PRS samples, the {10−12} tensile twinning was restrained in inner region of samples. The volume fraction of twins decreased with the increase of

PRS levels, which was supposed to be related to the decrease of c/a ratio. Detwinning behavior occurred in PRC samples in the outer region during bending. detwinning and twinning was a similar processes leading to a decrease of asymmetry of strain mechanisms between the outer and inner regions. Due to the decrease of tension/compression asymmetry, *k-value* decreased as well.

Acknowledgements

This work is supported by Fundamental Research Funds for the Central Universities (No. CDJZR13130081). Lifei Wang is grateful for financial support of the China Scholarship Council (CSC).

References

[1] Zhang H, Liu Y, Fan JF, Roven HJ, Cheng WL, Xu BS, et al. Microstructure evolution and mechanical properties of twinned AZ31 alloy plates at lower elevated temperature. J Alloys Compd 2014;615:687–92.

[2] Asgari H, Szpunar JA, Odeshi AG. Texture evolution and dynamic mechanical behavior of cast AZ magnesium alloys under high strain rate compressive loading. Mater Des 2014;61:26–34.

[3] Knezevic M, Levinson A, Harris R, Mishra RK, Doherty RD, Kalidindi SR. Deformation twinning in AZ31: influence on strain hardening and texture evolution. Acta Mater 2010;58:6230–42.

[4] Song B, Xin RL, Chen G, Zhang XY, Liu Q. Improving tensile and compressive properties of magnesium alloy plates by pre-cold rolling. Scripta Mater 2012;66:1061–4.

[5] Xin YC, Wang MY, Zeng Z, Nie MG, Liu Q. Strengthening and toughening of magnesium alloy by 10–12 extension twins. Scripta Mater 2012;66:25–8.

[6] Wang YN, Huang JC. The role of twinning and untwinning in yielding behavior in hot-extruded Mg–Al–Zn alloy. Acta Mater 2007;55:897–905.

[7] Zhang H, Huang GS, Wang LF, Li JH. Improved formability of Mg–3Al–1Zn alloy by pre-stretching and annealing. Scripta Mater 2012;67:495–8.

[8] Wang LF, Huang GS, Zhang H, Wang YX, Yin L. Evolution of springback and neutral layer of AZ31B magnesium alloy V-bending under warm forming conditions. J Mater Process Technol 2013;213:844–50.

[9] Zhang XP, Feng SF, Hong XT, Liu JQ. Orientation-related thickness effects on mechanical properties of hot extruded AZ31B magnesium alloy. Mater Des 2013;46:256–63.

[10] Patela HA, Chen DL, Bholea SD, Sadayappan K. Low cycle fatigue behavior of a semi-solid processed AM60B magnesium alloy. Mater Des 2013;49:456–64.

[11] Luo TJ, Yang YS, Tong WH, Duan QQ, Dong XG. Fatigue deformation characteristic of as-extruded AM30 magnesium alloy. Mater Des 2010;31:1617–21.

[12] AQSIQ Standard GB/T232-2010. Metallic materials-bending testing at ambient temperature. General administration of quality supervision, inspection and quarantine of the People's Republic of China; 2010.

[13] Zhang H, Jin W, Fan JF, Cheng WL, Roven HJ, Xu BS, et al. Grain refining and improving mechanical properties of a warm rolled AZ31 alloy plate. Mater Lett 2014;135:31–4.

[14] Kadiri HE, Kapil J, Oppedal AL, Hector LG, Agnew SR, Cherkaoui M, et al. The effect of twin–twin interactions on the nucleation and propagation of twinning in magnesium. Acta Mater 2013;61:3549–63.

[15] Kuo F, Huang TB. Formability of stamping magnesium-alloy AZ31 sheets. J Mater Process Technol 2003;142:643–7.

[16] Bruni C, Forcellese A, Gabrielli F, Simoncini M. Effect of temperature, strain rate and fibre orientation on the plastic flow behaviour and formability of AZ31 magnesium alloy. J Mater Process Technol 2010;210:1354–63.

[17] Huang GS, Wang LF, Zhang H, Wang YX, Shi ZY, Pan FS. Evolution of neutral layer and microstructure of AZ31B magnesium alloy sheet during bending. Mater Lett 2013;98:47–50.

[18] Sheng GM, Zhang GT, Yan C. Research of Bauschinger effect of AZ31 magnesium alloy. Rare Mater Eng 2011;40:616–9.

[19] Xu S, Liu TM, Chen HC, Miao ZC, Zhang Z, Zeng W. Reducing the tension–compression yield asymmetry in a hot-rolled Mg–3Al–1Zn alloy via multidirectional pre-compression. Mater Sci Eng A 2013;565:96–101.

[20] He JJ, Liu TM, Xu S, Zhang Y. The effects of compressive pre-deformation on yield asymmetry in hot-extruded Mg–3Al–1Zn alloy. Mater Sci Eng A 2013;579:1–8.

[21] Jabbari-Taleghani MA, Torralba JM. Hot workability of nanocrystalline AZ91 magnesium alloy. J Alloys Compd 2014;595:1–7.

[22] Wu W, Lee SY, Paradowska AM, Gao YF, Liaw PK. Twinning–detwinning behavior during fatigue-crack propagation in a wrought magnesium alloy AZ31B. Mater Sci Eng A 2012;556:278–86.

[23] Sarker D, Friedman J, Chen DL. Influence of pre-strain on de-twinning activity in an extruded AM30 magnesium alloy. Mater Sci Eng A 2014;605:73–9.